JOURNAL OF THEORETICAL AND APPLIED MECHANICS
51, 1, pp. 105-116, Warsaw 2013

A GENERALIZED UPPER BOUND SOLUTION FOR EXTRUSION OF BI-METALLIC RECTANGULAR CROSS-SECTION BARS THROUGH DIES OF ANY SHAPE

Heshmatollah Haghighat, Parvaneh Amjadian
Razi University, Mechanical Engineering Department, Kermanshah, Iran
e-mail: hhaghighat@razi.ac.ir

In this paper, a generalized upper bound solution is developed for extrusion of bi-metallic rectangular cross-section bars through dies of any shape. The internal, shearing and frictional power terms are derived and they are used in the upper bound model. By using the developed upper bound model, the extrusion pressures for two types of die shapes, an optimum wedge shaped die as a linear die profile and an optimum streamlined die shape as a curved die profile, are determined. The corresponding results for those two die shapes are also determined by using the finite element code and compared with the upper bound results. These comparisons show a good agreement.

Key words: extrusion, bimetal, plane strain, upper bound method, FEM

Nomenclature

b_c, b_s	–	widths of core and sleeve materials, respectively
dQ	–	differential volume flow
P	–	extrusion pressure
J^*	–	externally supplied power of deformation
L, L_o	–	length of die and initial bi-metallic billet length
m_1, m_2	–	friction factor between sleeve and die, and between core and sleeve
r, θ, z	–	cylindrical coordinate system
r_f, r_o	–	radial position of surfaces S_2 and S_4, and of surfaces S_1 and S_3
x	–	punch displacement
S	–	surface of integration
S_1-S_4	–	cylindrical surfaces of velocity discontinuity
t_{1f}, t_{2f}	–	half thickness of sleeve and core in final product
t_{1o}, t_{2o}	–	half thickness of sleeve and core in initial bar
$\dot{U}_r, \dot{U}_\theta, \dot{U}_z$	–	radial, angular and third components of velocity
V	–	volume of integration
V_f, V_o	–	velocity of final product and initial billet, respectively
$\dot{W}_f, \dot{W}_i, \dot{W}_s$	–	friction power losses along the wall, internal power of deformation and shear power losses along surface of velocity discontinuity, respectively
α	–	angle of line connecting initial to final point of die
γ	–	arbitrary angle on cylindrical surfaces S_1 and S_3
β	–	angle of interface in deformation zone
ΔV	–	velocity difference
$\dot{\varepsilon}_{rr}, \dot{\varepsilon}_{\theta\theta}, \dot{\varepsilon}_{zz}$	–	normal strain rate components in radial, angular and third directions
$\dot{\varepsilon}_{r\theta}, \dot{\varepsilon}_{rz}, \dot{\varepsilon}_{z\theta}$	–	shear strain rate components
η	–	local angle of die surface with respect to local radial velocity component

σ_c, σ_s – mean flow stress of core and sleeve material
$\psi(r), \psi_i(r)$ – angular position of die and interface as function of radial position

1. Introduction

Bimetals are components made up of two separate metallic units, each occupying a distinct position in the component. Bimetal components make possibility of combining properties of dissimilar metals. The compressive state of stress in extrusion and the possibility of producing metallurgical bonds between the two metals make this process a suitable choice for producing bimetal bars (Berski *et al.*, 2004). In this process, alike other metal forming processes, estimation and minimization of the extrusion pressure is important. The upper bound technique as an analytical method and the finite element method have been widely used for the analysis of the extrusion of bars made of mono-metal and bi-metallic materials. One of the limitations of most of the current FE solution schemes for metal forming is that they do not provide parametric analysis. Hence, any parametric investigation is usually done manually by changing one FE model to another until a feasible solution is obtained. Analytical solutions facilitate parametric study and can aid an FE modeler in seeking out optimal extrusion process conditions. After the upper bound model has determined the optimal die shapes, a finite element model has then been used to study the extrusion through dies with these optimal shapes.

A number of people have used the upper bound method and FEM to analyze the mono-metal and bimetal extrusion process through a variety of die shapes. Zimmerman and Avitzur (1970) modeled the mono-metal extrusion using the upper bound method with generalized shear boundaries. Osakada *et al.* (1973) described the hydrostatic extrusion of bi-metallic bars with hard cores through conical dies by the upper bound method. Nagpal (1974) developed velocity fields for axisymmetric mono-metal extrusions through arbitrarily shaped dies. Chen *et al.* (1979) used finite element analysis to examine the axisymmetric extrusion through conical dies. Avitzur (1983) summarized the factors that affect simultaneous flow of layers in the extrusion of a bimetal bar through conical dies. Tokuno and Ikeda (1991) verified the deformation in extrusion of composite bars by experimental and upper bound methods. Yang *et al.* (1999) studied the axisymmetric extrusion of composite bars through curved dies by experimental and upper bound methods. Sliwa (1997) described the plastic zones in the forward extrusion of metal composites by experimental and upper bound methods. Chitkara and Aleem (2001a,b) theoretically studied the mechanics of extrusion of axisymmetric bi-metallic tubes from solid circular bars using fixed mandrel with application of generalized upper bound and slab method analyses. They investigated the effect of different parameters such as the extrusion ratio, frictional conditions, and shape of the dies and the mandrels on the extrusion pressures. Kang *et al.* (2002) designed a die for the hot forward and backward extrusion process of Al-Cu clad composite by experimental investigations and FEM simulations. Hwang and Hwang (2002) studied the plastic deformation behavior within a conical die during composite bar extrusion by experimental and upper bound methods. Haghighat and Asgari (2011) proposed a generalized spherical velocity field for the bi-metallic tube extrusion process through dies of any shape. Haghighat and Amjadian (2011) developed velocity fields for the mono-metal plane strain extrusion through arbitrarily curved dies.

The purpose of this paper is to develop a generalized upper bound solution for flow of bi-metallic rectangular cross-section bars during extrusion through dies of any shape. Based on this model, for a given die shape and process parameters, the optimum die length and extrusion pressure are derived. The FEM simulation on the extrusion of a bi-metallic rectangular cross-section bar composed of a copper sleeve layer and an aluminum core layer is also conducted.

2. Upper bound analysis

Based on the upper bound theory, for a rigid-plastic Von-Misses material and amongst all the kinematically admissible velocity fields, the actual one that minimizes the power required for material deformation is expressed as

$$J^* = \frac{2}{\sqrt{3}}\sigma_0 \int_v \sqrt{\frac{1}{2}\dot{\varepsilon}_{ij}\dot{\varepsilon}_{ij}}\, dV + \frac{\sigma_0}{\sqrt{3}} \int_{S_V} |\Delta V|\, dS + m\frac{\sigma_0}{\sqrt{3}} \int_{S_f} |\Delta V|\, dS - \int_{S_t} T_i V_i\, dS \tag{2.1}$$

where σ_0 is the mean flow stress of the material, $\dot{\varepsilon}_{ij}$ the strain rate tensor, m the constant friction factor, V the volume of the plastic deformation zone, S_V and S_f the area of velocity discontinuity and frictional surfaces, respectively, S_t the area where tractions may occur, ΔV the amount of velocity discontinuity on the frictional and discontinuity surfaces and V_i and T_i are the velocity and tractions applied on S_t, respectively.

The extrusion of the bi-metallic rectangular cross-section bar through a die of arbitrary curved shape is modelled as shown in Figs. 1 and 2. An initially billet, made up two different ductile materials with the mean flow stresses σ_c and σ_s, is considered. The subscripts c and s denote the inner material, core, and outer material, sleeve, respectively. The material starts as a bar with the sleeve thickness $2t_{1o}$ and core thickness $2t_{2o}$ and it extrudes into a product of thicknesses $2t_{2f}$ and $2t_{1f}$ for the sleeve and core through a curved die, respectively. Because of the width of the core b_c and width of the sleeve b_s are long, $b_c \cong b_s \gg 2t_{1o}$, the process can be assumed as a plane strain extrusion.

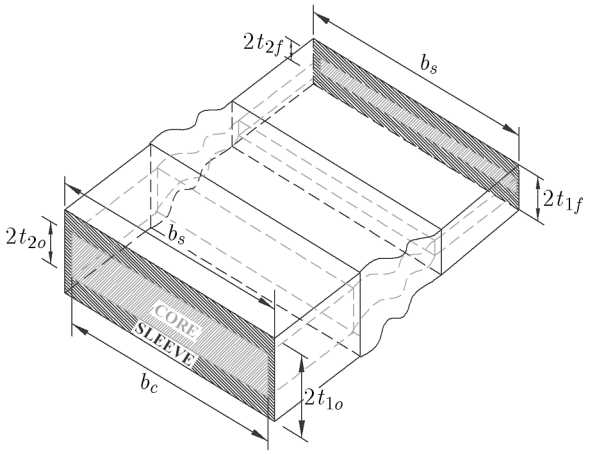

Fig. 1. The extrusion process of a bi-metallic rectangular cross-section billet through an arbitrarily curved die

To analyze the process, the material under deformation is divided into six zones, as shown in Fig. 2. The die surface, which is labeled as $\psi(r)$ in Fig. 2, is given in the cylindrical coordinate system (r, θ, z). The origin of the cylindrical coordinate system is located at the point O which is defined by the intersection of the midline with a line at the angle α that goes through the point where the die begins and the exit point of the die.

In zones I and II, the incoming materials are assumed to flow horizontally as a rigid body with velocity V_o. In zones V and VI, the extruded materials are assumed to flow horizontally as a rigid body with velocity V_f. Zones III and IV are the deformation regions, where the velocity is complex. These zones are surrounded by four velocity discontinuity surfaces S_1, S_2, S_3 and S_4. In addition to these surfaces, there are two frictional surfaces between the sleeve and container and the die surface and sleeve S_5. The surfaces S_1 and S_3 are located at a distance r_o from the origin, and the surfaces S_2 and S_4 are located at a distance r_f from the origin. The

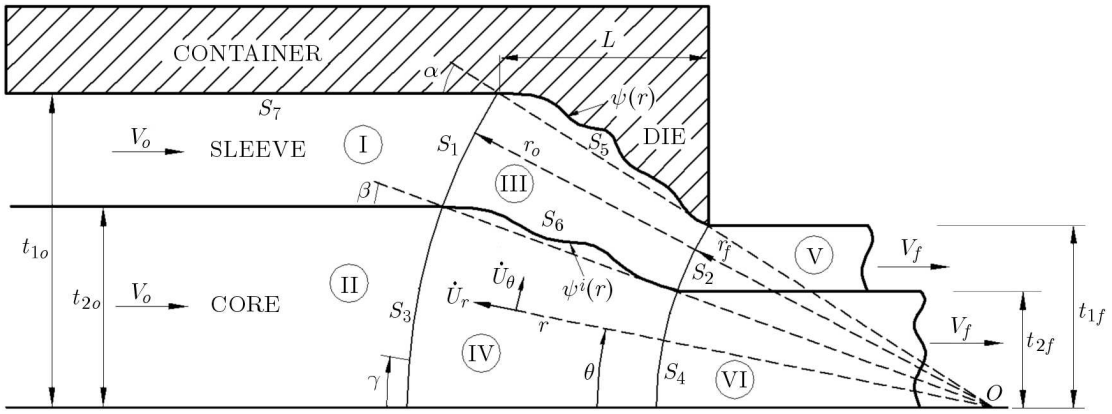

Fig. 2. Schematic diagram of a plane strain extrusion of a bi-metallic strip through a curved die and the cylindrical coordinate system

mathematical equations for radial positions of four velocity discontinuity surfaces S_1, S_3 and S_2, S_4 are given by

$$r_o = \frac{t_{1o} - t_{2o}}{\sin\alpha} \qquad r_f = \frac{t_{1f} - t_{2f}}{\sin\alpha} \tag{2.2}$$

where α is the angle of the line connecting the initial point of the curved die to the final point of the die and

$$\tan\alpha = \frac{t_{1o} - t_{1f}}{L} \tag{2.3}$$

where L denotes the die length. The interface surface between the inner and the outer materials is defined by $\psi_i(r)$, which is the angular position of the interface surface as a function of the radial distance from the origin. The angle β, shown in Fig. 2, is given by

$$\sin\beta = \frac{t_{2o}}{t_{1o}}\sin\alpha \tag{2.4}$$

2.1. Velocity field in the deformation zone

The first step in the upper bound analysis is to choose an admissible velocity field for the material undergoing plastic deformation. The velocity field that derives from incompressibility condition and satisfies the velocity boundary conditions is a kinematically admissible velocity field.

The velocity component in the radial direction within the deformation zone $\dot{U}_r$ can be obtained by assuming volume flow balance. In Fig. 2, the volume flow of the material across the S_1 and S_3 surface at the point (r_o, γ, z) in the radial direction is

$$dQ = -V_o\cos(\gamma)br_o\,d\gamma \tag{2.5}$$

The volume flow of the material in the radial direction at the point (r, θ, z) in the deformation zone is

$$dQ = \dot{U}_r br\,d\theta \tag{2.6}$$

Equating Eqs. (2.5) and (2.6), the radial velocity in the deformation zone is

$$\dot{U}_r = -V_o\frac{r_o}{r}\cos\gamma\frac{d\gamma}{d\theta} \tag{2.7}$$

Regarding the relationship between the angular positions γ, on the surfaces S_1 and S_3, and the angular position θ in the deformation zone and assuming proportional distances from the midline in the deformation zone (Gordon *et al.*, 2007), one obtains

$$\frac{\sin\gamma}{\sin\alpha} = \frac{\sin\theta}{\sin\psi} \tag{2.8}$$

where the angle ψ is the angular position of a point on the die profile.

Differentiating Eq. (2.8) yields

$$\cos\gamma\frac{d\gamma}{d\theta} = \sin\alpha\frac{\cos\theta}{\sin\psi} \tag{2.9}$$

Replacing Eqs. (2.9) into Eq. (2.7) gives the radial velocity component in the deformation zone as

$$\dot{U}_r = -V_o\frac{r_o}{r}\frac{\sin\alpha}{\sin\psi}\cos\theta \tag{2.10}$$

When the die shape reduces to a linear die profile, it has a single value (i.e. $\psi(r) = \alpha$) and Eq. (2.10) reduces to the velocity field proposed by Avitzur (1968) for the mono-metal plane strain extrusion through a wedge shaped die.

The full velocity field for the flow of the material in the deformation zones is obtained by invoking volume constancy. The volume constancy in cylindrical coordinate system is defined as

$$\dot{\varepsilon}_{rr} + \dot{\varepsilon}_{\theta\theta} + \dot{\varepsilon}_{zz} = 0 \tag{2.11}$$

where $\dot{\varepsilon}_{ii}$ is the normal strain rate component in the i-th direction. The strain rates components in cylindrical coordinates are defined as

$$\begin{aligned}
&\dot{\varepsilon}_{rr} = \frac{\partial\dot{U}_r}{\partial r} && \dot{\varepsilon}_{\theta\theta} = \frac{1}{r}\frac{\partial\dot{U}_\theta}{\partial\theta} + \frac{\dot{U}_r}{r} && \dot{\varepsilon}_{zz} = \frac{\partial\dot{U}_z}{\partial z}\\
&\dot{\varepsilon}_{r\theta} = \frac{1}{2}\Big(\frac{\partial\dot{U}_\theta}{\partial r} + \frac{1}{r}\frac{\partial\dot{U}_r}{\partial\theta} - \frac{\dot{U}_\theta}{r}\Big) && \dot{\varepsilon}_{\theta z} = \tfrac{1}{2}\Big(\tfrac{\partial\dot{U}_\theta}{\partial z} + \frac{1}{r}\frac{\partial\dot{U}_z}{\partial\theta}\Big) && \dot{\varepsilon}_{zr} = \frac{1}{2}\Big(\frac{\partial\dot{U}_r}{\partial z} + \frac{\partial\dot{U}_z}{\partial r}\Big)
\end{aligned} \tag{2.12}$$

For the plane strain extrusion (i.e. $\dot{U}_z = 0$), the full velocity field is obtained by placing $\dot{U}_r$, from Eq. (2.10) into Eqs. (2.11) and (2.12), solving for $\dot{U}_\theta$ and applying appropriate boundary conditions. The boundary conditions are as $\dot{U}_\theta|_{\theta=0} = 0$ for the midline and for the die surface $(\dot{U}_\theta/\dot{U}_r)|_{\theta=\psi} = r\partial\psi/\partial r$. Then, the velocity components can be given by

$$\dot{U}_r = -V_o\frac{r_o}{r}\frac{\sin\alpha}{\sin\psi}\cos\theta \qquad \dot{U}_\theta = -V_o r_o\frac{\sin\alpha}{\sin\psi}\frac{\partial\psi}{\partial r}\cot\psi\sin\theta \qquad \dot{U}_z = 0 \tag{2.13}$$

Based on the established velocity field, the strain rate field for the deformation zone can be obtained by Eqs. (2.12) as

$$\begin{aligned}
\dot{\varepsilon}_{rr} &= -\dot{\varepsilon}_{\theta\theta} = V_o\frac{r_o}{r^2}\frac{\sin\alpha}{\sin\psi}(1 + r\frac{\partial\psi}{\partial r}\cot\psi)\cos\theta\\
\dot{\varepsilon}_{r\theta} &= \frac{1}{2}V_o\frac{r_o}{r^2}\frac{\sin\alpha}{\sin\psi}\Big[1 - r^2\cot\psi\frac{\partial^2\psi}{\partial r^2} + r^2(1+\cot^2\psi)\Big(\frac{\partial\psi}{\partial r}\Big)^2 + \cot^2\psi\Big(\frac{\partial\psi}{\partial r}\Big)^2\\
&\quad + r\cot\psi\frac{\partial\psi}{\partial r}\Big]\sin\theta\\
\dot{\varepsilon}_{zz} &= \dot{\varepsilon}_{\theta z} = \dot{\varepsilon}_{zr} = 0
\end{aligned} \tag{2.14}$$

With the strain rate field and the velocity field, the standard upper bound method can be implemented. This upper bound model involves calculating the internal power of deformation over the deformation zone volume, calculating the shear power losses over the four surfaces of velocity discontinuity, and the frictional power losses between the sleeve and the die and between the sleeve and the container.

2.2. Internal power of deformation

The internal power of deformation in the upper bound model is

$$\dot{W}_i = \frac{2}{\sqrt{3}}\sigma_0 \int_v \sqrt{\frac{1}{2}\dot{\varepsilon}_{ij}\dot{\varepsilon}_{ij}}\, dV \tag{2.15}$$

The internal power of zones I, II, V and VI are zero, and the equation to calculate the internal power of deformation in zone III is

$$\dot{W}_{iIII} = \frac{2\sigma_s}{\sqrt{3}} b \int_{r_f}^{r_o} \int_{\psi_i(r)}^{\psi(r)} \sqrt{\frac{1}{2}\dot{\varepsilon}_{rr}^2 + \frac{1}{2}\dot{\varepsilon}_{\theta\theta}^2 + \dot{\varepsilon}_{r\theta}^2}\, r\, d\theta\, dr \tag{2.16}$$

where σ_s is the mean flow stress of the sleeve material, and is determined by

$$\sigma_s = \frac{1}{\varepsilon}\int_0^{\varepsilon} \sigma\, d\varepsilon \qquad \varepsilon = \ln\frac{t_{1o} - t_{2o}}{t_{1f} - t_{2f}} \tag{2.17}$$

and $\psi_i(r)$ is the angular position of the interface surface as a function of the radial distance from the origin O, and is given by

$$\psi_i(r) = \sin^{-1}\Big[\frac{\sin\beta}{\sin\alpha}\sin\psi(r)\Big] \tag{2.18}$$

The general equation to calculate the internal power of deformation in zone IV is determined as

$$\dot{W}_{iIV} = \frac{2\sigma_c}{\sqrt{3}} b \int_{r_f}^{r_o} \int_{0}^{\psi_i(r)} \sqrt{\frac{1}{2}\dot{\varepsilon}_{rr}^2 + \frac{1}{2}\dot{\varepsilon}_{\theta\theta}^2 + \dot{\varepsilon}_{r\theta}^2}\, r\, d\theta\, dr \tag{2.19}$$

where σ_c is the mean flow stress of core material and is given by

$$\sigma_c = \frac{1}{\varepsilon}\int_0^{\varepsilon} \sigma\, d\varepsilon \qquad \varepsilon = \ln\frac{t_{2o}}{t_{2f}} \tag{2.20}$$

2.3. Shear power losses

The equation for the power losses along the shear surface of velocity discontinuity is

$$\dot{W}_S = \frac{\sigma_0}{\sqrt{3}} \int_{S_v} |\Delta V|\, dS \tag{2.21}$$

The shear power losses along the velocity discontinuity surfaces S_1, S_2, S_3 and S_4 can be given by

$$\begin{aligned}
\dot{W}_{S1} &= \frac{\sigma_s}{\sqrt{3}} V_o r_o b \int_{\beta}^{\alpha} \Big(1 + r_o \frac{\partial \psi}{\partial r}\Big|_{r=r_o} \cot\alpha\Big) \sin\theta \, d\theta \\
\dot{W}_{S2} &= \frac{\sigma_s}{\sqrt{3}} V_o r_o b \int_{\beta}^{\alpha} \Big(1 + r_o \frac{t_o}{t_f} \frac{\partial \psi}{\partial r}\Big|_{r=r_f} \cot\alpha\Big) \sin\theta \, d\theta \\
\dot{W}_{S3} &= \frac{\sigma_c}{\sqrt{3}} V_o r_o b \int_{0}^{\beta} \Big(1 + r_o \frac{\partial \psi}{\partial r}\Big|_{r=r_o} \cot\alpha\Big) \sin\theta \, d\theta \\
\dot{W}_{S4} &= \frac{\sigma_c}{\sqrt{3}} V_o r_o b \int_{0}^{\beta} \Big(1 + r_o \frac{t_o}{t_f} \frac{\partial \psi}{\partial r}\Big|_{r=r_f} \cot\alpha\Big) \sin\theta \, d\theta
\end{aligned} \tag{2.22}$$

2.4. Friction power losses

The general equation for the friction power losses for the surface with a constant friction factor m_1 is

$$\dot{W}_f = m_1 \frac{\sigma_0}{\sqrt{3}} \int_{S_f} |\Delta V| \, dS \tag{2.23}$$

For the die surface S_5

$$dS_5 = \sqrt{1 + \Big(r \frac{\partial \psi}{\partial r}\Big)^2} \, dr \qquad |\Delta V| = |\dot{U}_r \cos\eta + \dot{U}_\theta \sin\eta|_{\theta=\psi} \tag{2.24}$$

where η is the local angle of the die surface with respect to the local radial velocity component and

$$\cos\eta = \frac{1}{\sqrt{1 + \Big(r \frac{\partial \psi}{\partial r}\Big)^2}} \qquad \sin\eta = \frac{r \frac{\partial \psi}{\partial r}}{\sqrt{1 + \Big(r \frac{\partial \psi}{\partial r}\Big)^2}} \tag{2.25}$$

The frictional power losses along the die surface are calculated as

$$\dot{W}_{f5} = \frac{\sigma_s}{\sqrt{3}} m_1 V_0 b r_{1o} \int_{r_f}^{r_o} \frac{\sin\alpha}{r \tan\psi} \Big[1 + \Big(r \frac{\partial \psi}{\partial r}\Big)^2\Big] \, dr \tag{2.26}$$

where m_1 is the constant friction factor between the sleeve and die.

The frictional power losses along the container surface S_7 can be given by

$$\dot{W}_{f7} = \frac{\sigma_s}{\sqrt{3}} m_1 V_o b (L_o - x) \tag{2.27}$$

where x is the displacement of the punch and L_o is the initial bi-metallic billet length.

Based on the upper bound model, the total power needed for a bi-metallic plane strain extrusion process can obtained by summing the internal power and the power dissipated on all frictional and velocity discontinuity surfaces. Then, the total upper bound solution for the extrusion pressure is given by

$$P_e = \frac{\dot{W}_{iIII} + \dot{W}_{iIV} + \dot{W}_{s1} + \dot{W}_{s2} + \dot{W}_{s3} + \dot{W}_{s4} + \dot{W}_{f5} + \dot{W}_{f7}}{b t_{1o} V_o} \tag{2.28}$$

A MATLAB program has been implemented for the previously derived equations and has been used to study the plastic deformation for different die shapes and friction conditions. It includes the parameter L, the die length that should be optimized.

3. Results and discussion

To make a comparison with the developed model, a bimetal bar composed of aluminium as the core layer and copper as the sleeve layer is used. The flow stresses for copper and aluminium in room temperature are obtained as (Hwang and Hwang, 2002)

$$\sigma_{Al} = 189.2\varepsilon^{0.239}\,\text{MPa} \qquad \sigma_{Cu} = 335.2\varepsilon^{0.113}\,\text{MPa} \tag{3.1}$$

Friction factors $m_1 = 0.2$ and $m_2 = 0.9$, $t_{1o} = 10\,\text{mm}$, $t_{2o} = 6\,\text{mm}$, $t_{1f} = 7\,\text{mm}$ are adopted during the analytical solution and FEM simulation.

The developed upper bound model can be used for the bi-metallic plane strain extrusion through dies of any shape if the die profile is expressed as an equation of $\psi(r)$. Two types of die shapes are examined in the present investigation. The first die shape is wedge shaped die as a linear die profile. This profile has a single constant value, i.e. $\psi(r) = \alpha$. The second die shape is taken from the work by Yang and Han (1987). They created a streamlined die shape as a fourth-order polynomial whose slope is parallel to the axis at both entrance and exit. The die shape of Yang and Han (1987) was expressed in the cylindrical coordinate system.

In Fig. 3, the extrusion pressure of the wedge shaped die and the Yang and Han die shape obtained from the upper bound method are compared with each other. The extrusion pressure of Yang and Han die shape is lower than that of conical die. Because this curved die has a smooth transition at the die entrance and exit, the shearing in the velocity discontinuity surfaces is zero. At a die length called the optimum die length, the extrusion pressure is minimized. As shown in Fig. 3, the optimum die length in the case of the wedge shaped die is 7.9 mm, and in the case of Yang and Han die shape is of 10.7 mm.

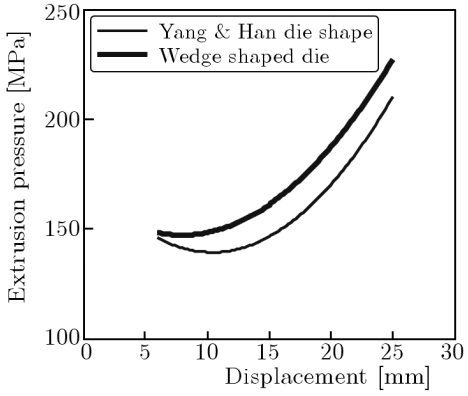

Fig. 3. Comparison between the analytical extrusion pressure values versus die length for the wedge shaped die and Yang and Han die shape

The extrusion process is simulated by using the finite element code ABAQUS. Two die shapes are used in simulations: (a) optimum wedge shaped die with 7.9 mm die length and (b) optimum Yang and Han die with 10.7 mm die length. Considering the symmetry in geometry, plane strain models are used for FEM analyses. In each case, the whole model is meshed with CAX4R elements. The punch and the die are modeled as rigid materials. The die model is fixed by applying displacement constraint on its nodes, while the punch model is loaded by specifying displacement in the axial direction. Figure 4a illustrates the mesh used to analyze the

deformation of the optimum Yang and Han die shape. Deformed models of the sleeve and core are shown in Fig. 4b. This figure shows that aluminum leaves the deformation zone sooner than copper. Since the flow stress of aluminum is lower than that of copper, the former extrudes first. As the applied stress increases the flow stress of copper, simultaneous flow of the two metals continues.

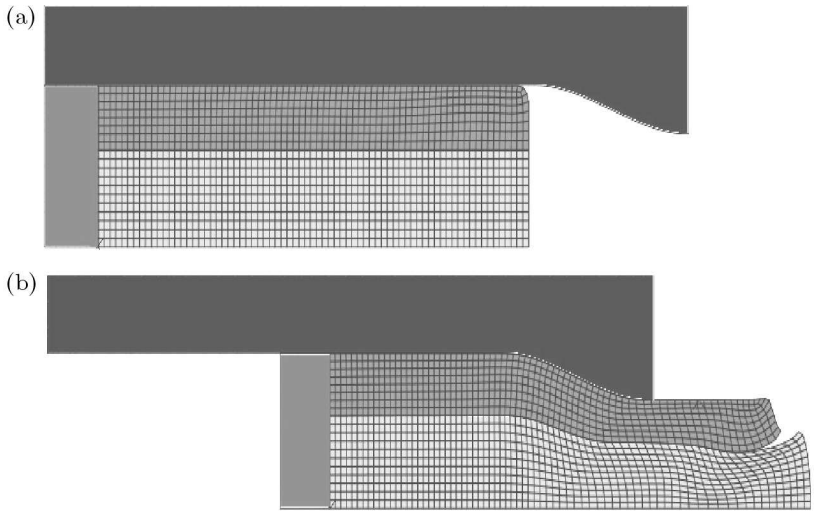

Fig. 4. (a) Finite element mesh and (b) deformed mesh in the bi-metallic plane strain extrusion process

In Figs. 5a and 5b, the extrusion pressure variation during the whole extrusion process obtained from the upper bound solution are compared with the FEM for the wedge shaped die and Yang and Han die shape having 8 mm and 11 mm die lengths, respectively. The results show a good agreement between the upper bound data and the FEM results. As shown in these figures, at the early stage of extrusion, an unsteady state deformation occurs, and the materials have not yet filled up the cavity of the die completely.

Thus, the extrusion pressure increases as the extrusion process proceeds. After the materials have filled up the cavity of the die completely, the extrusion pressure decreases gradually. The gradual decrease in the load-displacement curves is due to decreasing of the frictional surface area in the container as the punch is advanced. The results show a good agreement between the analysis and FEM results. As shown in Figs. 5a,b, the analytically predicted pressure is about 14% higher than the FEM result, which is due to the nature of the upper bound theory.

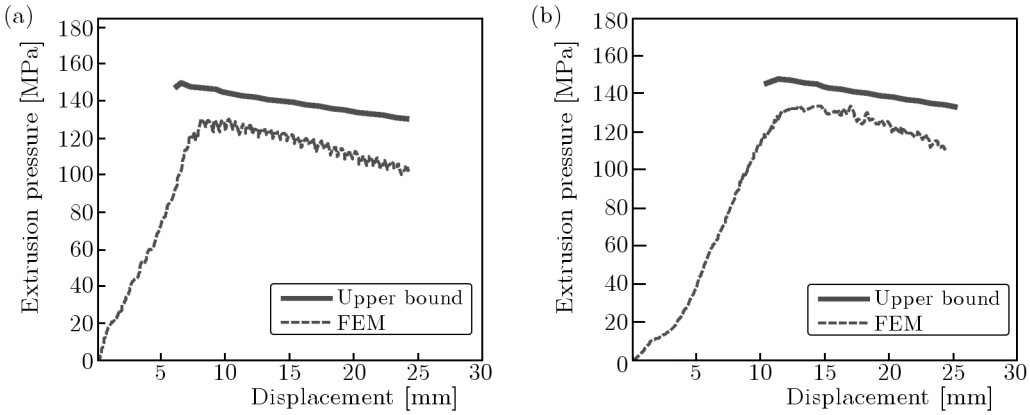

Fig. 5. Comparison of analytical and FEM extrusion pressure-displacement curves for the wedge shaped die (a) and for the Yang and Han die shape (b)

The effect of die length on the extrusion pressure for different values of the friction factor is shown in Fig. 6. As expected, for a given value of the friction factor, the extrusion pressure is minimized in the optimum die length. It is observed that the optimum die length decreases when the shearing friction factor increases. This figure, also, shows that an increase in the friction factor tends to increase the extrusion pressure.

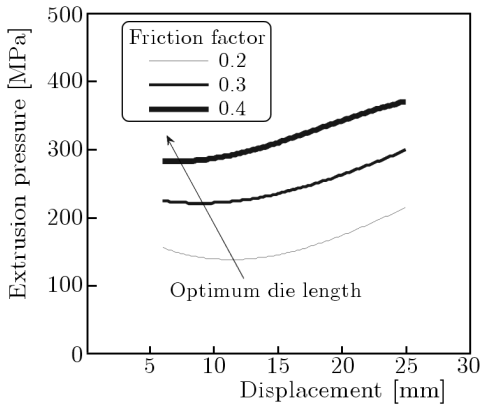

Fig. 6. The effect of die length on the extrusion pressure for different values of the friction factor for the Yang and Han die shape

Since the developed upper bound solution is faster than FEM analysis, it can be very beneficial in studying the influence of multiple variables on the bi-metallic rectangular cross-section bar extrusion process and for a given die shape, it can be used for finding the optimum die length which minimizes the extrusion pressure.

4. Conclusions

In this research, a generalized velocity field for use in the upper bound model of the extrusion process of the bi-metallic rectangular cross-section bar through dies of any shape was developed. By using the developed upper bound model, optimum die lengths for the wedge shaped die and also for the Yang and Han die shape have been determined. The extrusion pressure for these two dies has been found by using the finite element code, ABAQUS, and compared with analytical results. These comparisons show a good agreement, and the extrusion pressure of the Yang and Han die shape was lower than in the wedge shaped die.

The developed upper bound model can be used for fast estimation of the extrusion pressure of bi-metallic rectangular cross-section bars through dies of any shape and for a given die shape and process parameters. It can be used for finding the optimum die length which minimizes the extrusion pressure.

References

1. Avitzur B., 1968, *Metal Forming: Processes and Analysis*, McGraw-Hill, New York

2. Avitzur B., 1983, *Handbook of Metal-Forming Processes*, Wiley, New York

3. Berski S., Dyja H., Banaszek G., Janik M., 2004, Theoretical analysis of bimetal bar extrusion process in double reduction dies, *Journal of Materials Processing Technology*, **154**, 153-183

4. Chen C.C., Oh S.I., Kobayashi S., 1979, Ductile fracture in axisymmetric extrusion and drawing - Part 1: deformation mechanics of extrusion and drawing metal, *Transactions of the ASME, Journal of Engineering for Industry*, **101**, 23-35

5. Chitkara N.R., Aleem A., 2001a, Extrusion of axi-symmetric bi-metallic tubes from solid circular bars: application of a generalized upper bound analysis and some experiments, *International Journal of Mechanical Sciences*, **43**, 2833-2856

6. Chitkara N.R., Aleem A., 2001b, Extrusion of axi-symmetric bi-metallic tubes: some experiments using hollow bars and the application of a generalized slab method of analysis, *International Journal of Mechanical Sciences*, **43**, 2857-2882

7. Gordon W.A, Van Tyne C.J., Moon Y.H., 2007a, Axisymmetric extrusion through adaptable dies – Part 1: Flexible velocity fields and power terms, *International Journal of Mechanical Sciences*, **49**, 86-95

8. Gordon W.A., Van Tyne C.J., Moon Y.H., 2007b, Axisymmetric extrusion through adaptable dies - Part 3: Minimum pressure streamlined die shapes, *International Journal of Mechanical Sciences*, **49**, 104-115

9. Haghighat H., Amjadian P., 2011, A generalized velocity field for plane strain extrusion through arbitrarily curved dies, *Transactions of the ASME, Journal of Manufacturing Science and Engineering*, **133**, 041006

10. Haghighat H., Asgari G.R., 2011, A generalized spherical velocity field for bi-metallic tube extrusion through dies of any shape, *International Journal of Mechanical Sciences*, **53**, 248-253

11. Hwang Y.M., Hwang T.F., 2002, An investigation into the plastic deformation behavior within a conical die during composite bar extrusion, *Journal of Materials Processing Technology*, **12**, 226-233

12. Kang C.G., Jung Y.J., Kwon H.C., 2002, Finite element simulation of die design for hot extrusion process of Al/Cu clad composite and its experimental investigation, *Journal of Materials Processing Technology*, **124**, 49-56

13. Nagpal V., 1974, General kinematically admissible velocity fields for some axisymmetric metal forming problems, *Transactions of the ASME, Journal of Engineering for Industry*, **96**, 1197-1201

14. Osakada K., Limb M., Mellor P.B., 1973, Hydrostatic extrusion of composite bars with hard cores, *International Journal of Mechanical Sciences*, **15**, 291-307

15. Sliwa R., 1997, Plastic zones in the extrusion of metal composites, *Journal of Materials Processing Technology*, **67**, 29-35

16. Tokuno H., Ikeda K., 1991, Analysis of deformation in extrusion of composite bars, *Journal of Materials Processing Technology*, **26**, 323-335

17. Yang D.Y., Han C.H., 1987, A new formulation of generalized velocity field for axisymmetric forward extrusion through arbitrarily curved dies, *Transactions of the ASME, Journal of Engineering for Industry*, **109**, 161-168

18. Yang D.Y., Kim Y.G., Lee C.M., 1999, An upper-bound solution for axisymmetric extrusion of composite bars through curved dies, *International Journal of Mechanical Sciences*, **31**, 565-575

19. Zimmerman Z., Avitzur B., 1970, Metal flow through conical converging diesa lower upper bound approach using generalized boundaries of the plastic zone, *Transactions of the ASME, Journal of Engineering for Industry*, **92**, 119-129

Uogólnione rozwiązanie ograniczenia górnego problemu wytłaczania bimetalowych belek o przekroju prostokątnym za pomocą tłoczników o dowolnym kształcie

Streszczenie

W pracy wyprowadzono uogólnione rozwiązanie ograniczenia górnego problemu wytłaczania bimetalowych belek o przekroju prostokątnym za pomocą tłoczników o dowolnym kształcie. Wyznaczono wyrażenia potęgowe opisujące wewnętrzne, ścinające oraz tarciowe obciążenia i zastosowano je w modelu matematycznym omawianego zagadnienia. Zaproponowana metoda badań pozwoliła na określenie nacisku podczas wytłaczania elementów przy użyciu dwóch typów tłocznika – optymalnego klinowego o profilu liniowym oraz tłocznika o zarysie krzywoliniowym, opływowym. W obydwu przypadkach obliczenia porównano z wynikami uzyskanymi z metody elementów skończonych. Porównanie to wykazało dobrą zgodność rozwiązania ograniczenia górnego z rezultatami MES.

Manuscript received January 5, 2012; accepted for print March 26, 2012